2024 IEEE International Conference on Robotics and Automation (ICRA 2024)
May 13-17, 2024. Yokohama, Japan

Accelerating Robotic Picking of Rigid Objects with a Compliant Pneumatic Gripper and an Impact-Aware Trajectory Plan

Frederik Ostyn[1], Bram Vanderborght[2] and Guillaume Crevecoeur[1]

***Abstract*— Industrial robots are capable of moving at high speed. Each time they come into contact with their environment, e.g. to pick up an object, they decelerate to a near standstill. A solution involving a compliant pneumatic gripper and adapted trajectory plan is presented to initiate contact at a higher speed while remaining within hardware limits. By adding overload clutches in either the robot arm or gripper, tolerance to errors is provided. The key parameters such as gripper compliance and maximum allowed initial impact velocity are identified. Results show that by properly optimizing these parameters, robot picking of rigid objects can be accelerated. The complete high-speed picking solution is experimentally verified. A time reduction of 16% was obtained when making contact at 0.65 m/s.**

I. INTRODUCTION

Industrial robots move at ever increasing speeds. However, the moment contact with the environment is to be made, they have to decelerate to a near standstill. Impact is to be avoided as the current hard- and software is not collision tolerant nor impact-aware. Upon completion of the task involving contact, e.g. when picking an object, the robot has to accelerate again. The phase involving contact is hence the bottleneck, e.g. in a pick-and-place operation. Decelerating and accelerating is moreover not energy-efficient.

An impact-aware robot is capable of contacting an object at non-zero speeds within certain hardware limits. Dehio *et al.* presented a Model Predictive Controller (MPC) to maximize the intentional impact velocity within a feasible, robot-safe level assuming the impact will occur in the next time step [1]. The MPC generates a desired next time step velocity which is tracked by a velocity controller. Upon impact detection, the velocity controller switches to admittance control to track a desired force implied on the object. They extended this work to a dual arm setup in [2].

Beside impact velocity, also the pose and orientation of the robot determine the severity of the impact. They shape the impacting reflected mass along the collision direction [3], [4]. Tassi *et al.* therefore considered maximizing the dynamic impact measure in order to orient the robot to distribute the peak joint torque during rigid impacts [5]. They implemented this as a second priority in a hierarchical quadratic program with the robot's closed loop inverse kinematics as strict priority.

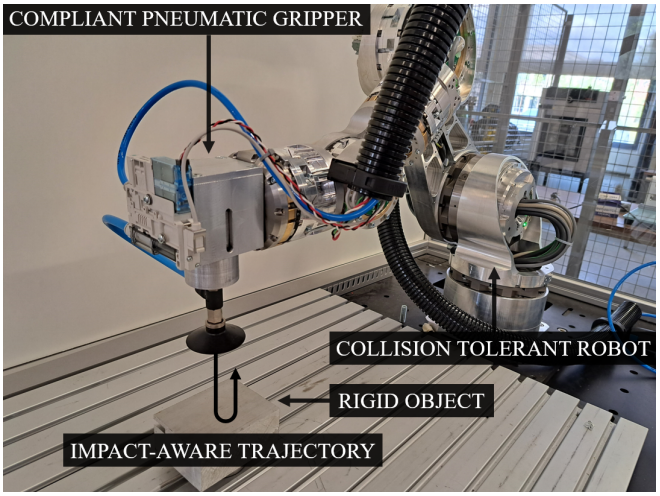

Fig. 1: Picking of a rigid object with a compliant pneumatic gripper. The compliance allows to accelerate the picking operation as contact can be made at non-zero speed.

Impact-aware controllers often rely on soft, deformable end-effector pads. They act as a mechanical low-pass filter reducing the maximum impact force. Besides adapting to the shape of the object [6], [7], compliant grippers can hence play an important role in accelerating phases involving contact. Compliant pads also reduce velocity jumps associated with rigid impact [8] that complicate the control problem [9]. Consequently, contact compliance is beside impact velocity and pose an important parameter influencing the collision event.

The gripper compliance may not be sufficient in case of a higher collision force than anticipated. An overload clutch [10], [11] that decouples upon unintentional high impact may be added to avoid hardware damage. It acts as a discrete variable stiffness mechanism. In nominal operation, the gripper compliance reduces the maximum impact force of intentional collisions. Upon unintensional impact, the clutch decouples, increasing the compliance considerably and hence protecting the hardware.

In this paper, we investigate how to accelerate a robotic pick-and-place operation if a compliant pneumatic gripper is used as shown in Fig. 1. The core idea is to add compliance in between the object and the robot arm. The object is then impacted at maximum speed without hardware damage and compresses the additional compliant device. The resulting

This work was supported by the FWO project 'Safe and collision-tolerant hybrid high-speed collaborative robots' under grant G0A9623N.

[1]F. Ostyn and G. Crevecoeur are with the Department of Electromechanical, Systems and Metal Engineering, Ghent University, 9000 Ghent; and with the Core Lab MIRO, Flanders Make (e-mail: Frederik.ostyn@ugent.be).

[2]B. Vanderborght is with the Robotics and Multibody Mechanics (R&MM) Research Group, Vrije Universiteit Brussel (VUB); with Imec and with the Core Lab R&MM, Flanders Make.

collision force is used to decelerate the robot arm. The compliant device stores part of the impact energy which is released when the arm starts to accelerate away from the impact, e.g. after pneumatically gripping the object. Overall, by impacting the object at non-zero speed, the complete pick-and-place operation is accelerated as will be shown. In case the robot is fitted with overload clutches, anomalies that result in a higher than anticipated collision force can be taken care of, avoiding hardware damage. Compared to grippers like [12], [13] and [14] which are also impact-aware and collision tolerant, the presented pneumatic gripper effectively harnesses the energy of the collision to speed up the picking operation.

The contributions of this paper are the time reduction when impacting the object at higher than zero speed with a compliant gripper with respect to making contact at standstill with a rigid gripper. Secondly, the key design parameters such as compliance and maximum impact velocity are identified as well as guidelines to choose them optimally. The presented approach is also validated experimentally, using a custom designed compliant pneumatic gripper. A high-speed picking operation is compared with a benchmark. In a third experiment, an anomaly triggers decoupling of an overload clutch, demonstrating the collision tolerance of the solution.

The article continues by presenting a pick-and-place trajectory with rigid pneumatic gripper as benchmark in Section II. Next, a high-speed picking alternative with shorter execution time is presented in Section III. Both are compared experimentally in Section IV. Finally, Section V concludes this paper.

II. BENCHMARK

A conventional robotic pick-and-place operation consists of the following phases, also shown in Fig. 2:

1) Start from zero velocity, speed up towards the object.
2) Reduce the speed to zero, prior to contacting the object.
3) Wait until the object is gripped, e.g. until vacuum is achieved in case of a pneumatic gripper.
4) Start accelerating towards the end position.
5) Decelerate until the end position is reached at zero speed.

Different trajectory profiles exist to realize the approaching and retracting motion. The fastest option is to use parabolic blends, applying maximum acceleration or deceleration. We assume that the robot starts at zero velocity and initial position q_0 and accelerates at the maximum allowed joint acceleration $\ddot{q}_{\max}$ to reach an intermittent joint velocity $\dot{q}_i$ at time instant t_i

$$\begin{cases} q_i = q_0 + \ddot{q}_{\max} t_i^2/2 \\ \dot{q}_i = \ddot{q}_{\max} t_i \end{cases} \tag{1}$$

to then decelerate to standstill prior to making contact with the object to be picked:

$$\begin{cases} q_{\text{pick}} = q_i + \dot{q}_i(t_{\text{pick}} - t_i) - \ddot{q}_{\max}(t_{\text{pick}} - t_i)^2/2 \\ \dot{q}_{\text{pick}} = \dot{q}_i - \ddot{q}_{\max}(t_{\text{pick}} - t_i) \end{cases} \tag{2}$$

at

$$t_{\text{pick}} = 2\sqrt{\frac{q_{\text{pick}} - q_0}{\ddot{q}_{\max}}} \tag{3}$$

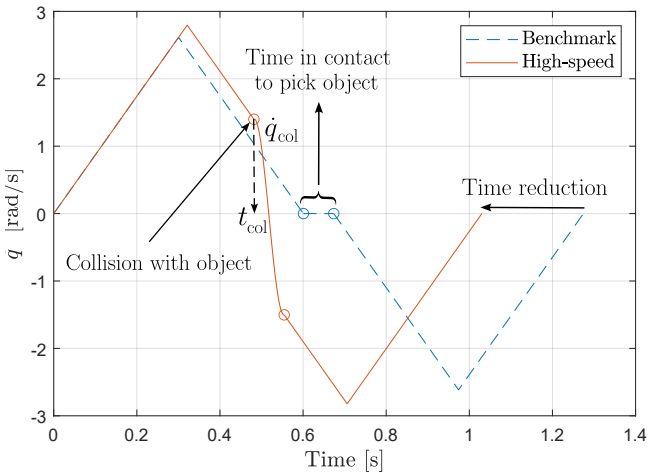

Fig. 2: Velocity profile during a picking operation. Shown are a benchmark in dashed line with contact made at zero velocity and a faster, high-speed variant where a compliant gripper collides with the object.

After gripping the object, e.g. pneumatically, the robot retracts using a similar motion profile as defined in Eqs. (1–2).

III. HIGH-SPEED PICKING

If the gripper allows to contact the object at non-zero speeds, the complete pick-and-place operation can be sped up. The robot does not have to decelerate up to standstill prior to making contact with the object, to then accelerate again when retracting. In the following, we investigate how to alter the robot's path to minimize the time required to perform the pick-and-place operation. We identify key parameters such as contact impedance and impact velocity and derive equations to choose them optimally.

A. Compliant pneumatic gripper

In order to allow contact with the object at non-zero speed, the gripper is made compliant. A custom pneumatic gripper design in shown in Fig. 3. A housing is fixed to the robot's end effector flange. The housing allows a piston with pneumatic suction cup to move up and down counteracting a set of compression springs. The springs act as a mechanical low-pass filter. They delay and reduce the maximum impact force when contact with the object is made at non-zero speed. They store the collision energy and release it when the arm retracts, increasing also the energy efficiency. An ejector vacuum pump with electric switch is mounted on the housing to build a vacuum and pick up an object or release the object if switched off. Compliant hardware is a necessary, but not sufficient condition to realize high-speed picking. An impact-aware trajectory plan is also required.

B. Pick-and-place trajectory plan and control strategy

We assume that the robot starts at zero velocity from a position q_0 that allows for every joint to accelerate at least up to $\dot{q}_{\text{col}} \neq 0$ m/s. Stated otherwise, the maximum joint

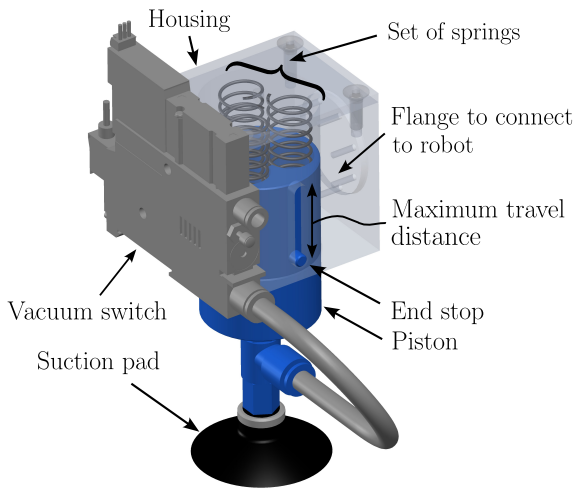

Fig. 3: Overview of the compliant pneumatic gripper design. A suction pad is mounted on a piston that slides in a housing, counteracting a set of springs. The springs allow to impact the object with the gripper at non-zero speed. The collision energy is stored and released again to accelerate the robot arm when retracting with the object. Such a compliant gripper design consequently allows to speed up robotic picking of objects.

acceleration $\ddot{q}_{\max}$ is sufficiently high to either reach the desired joint impact velocity $\dot{q}_{\text{col}}$ directly while accelerating at the maximum joint acceleration $\ddot{q}_{\max}$:

$$\begin{cases} q_{\text{col}} = q_0 + \ddot{q}_{\max} t_{\text{col}}^2/2 \\ \dot{q}_{\text{col}} = \ddot{q}_{\max} t_{\text{col}} \end{cases} \tag{4}$$

or by accelerating first to a higher intermittent joint velocity $\dot{q}_i > \dot{q}_{\text{col}}$

$$\begin{cases} q_i = q_0 + \ddot{q}_{\max} t_i^2/2 \\ \dot{q}_i = \ddot{q}_{\max} t_i \end{cases} \tag{5}$$

to then decelerate until the desired collision velocity is reached:

$$\begin{cases} q_{\text{col}} = q_i + \dot{q}_i(t_{\text{col}} - t_i) - \ddot{q}_{\max}(t_{\text{col}} - t_i)^2/2 \\ \dot{q}_{\text{col}} = \dot{q}_i - \ddot{q}_{\max}(t_{\text{col}} - t_i) \end{cases} \tag{6}$$

The maximum speed is reached prior to impact at time t_i

$$t_i = \frac{1}{2}\left(\frac{\dot{q}_{\text{col}}}{\ddot{q}_{\max}} + t_{\text{col}}\right) \tag{7}$$

with

$$t_{\text{col}} = -\frac{\dot{q}_{\text{col}}}{\ddot{q}_{\max}} + \sqrt{2\left(\frac{\dot{q}_{\text{col}}}{\ddot{q}_{\max}}\right)^2 + 4\frac{q_{\text{col}} - q_0}{\ddot{q}_{\max}}} \tag{8}$$

which reduces to Eq. (3) if $\dot{q}_{\text{col}} = 0$. Note that $t_{\text{col}} \leq t_{\text{pick}}$ and the higher $\dot{q}_{\text{col}}$, the higher the potential reduction in approach time.

In case of multiple rotating axes, at least one of the axes will limit the minimum time to collision t_{col}. We therefore calculate $t_{\text{col,i}}$ for every rotating joint to then choose $t_{\text{col}} = \max_i \{t_{\text{col,i}}\}$. Next, use Eq. (8) to adjust (reduce) the maximum accelerations of every axis $j \neq i$. Alternatively, a constant velocity portion could be added while maintaining maximum acceleration as in a Linear Segments with Parabolic Blends (LSPB) trajectory.

C. Impact model and its key parameters

The robot dynamics can be modeled via the Euler-Lagrange equations reduced to the link side

$$\mathbf{D}(\mathbf{q})\ddot{\mathbf{q}} + \mathbf{h}(\mathbf{q}, \dot{\mathbf{q}}) = \boldsymbol{\tau}_m + \mathbf{J}_v^T(\mathbf{q})\mathbf{f}_{\text{ext}} \tag{9}$$

with positive definite inertia matrix $\mathbf{D}(\mathbf{q}) \in \mathbb{R}^{n\times n}$ and $\mathbf{h}(\mathbf{q}, \dot{\mathbf{q}}) \in \mathbb{R}^{n\times 1}$ modeling the centrifugal and coreolis term, as well as the gravitational and joint friction term if present. An external force applied on the gripper $\mathbf{f}_{\text{ext}}$ results in joint torque $\mathbf{J}_v^T(\mathbf{q})\mathbf{f}_{\text{ext}}$ with $\mathbf{J}_v(\mathbf{q})$ the velocity Jacobian.

Instead of using the full state joint space dynamics, we study the collision along the direction of impact. Define $\mathbf{u}$ the unit vector along this direction. The reflected robot mass along $\mathbf{u}$ can be derived based on expressions for the kinetic energy in joint versus (Cartesian) task space:

$$m_u(\mathbf{q}) = \left[\mathbf{u}^T \boldsymbol{\Lambda}_v(\mathbf{q})^{-1}\mathbf{u}\right]^{-1} \tag{10}$$

with $\boldsymbol{\Lambda}_v(\mathbf{q})$ the translational Cartesian mass matrix

$$\boldsymbol{\Lambda}_v(\mathbf{q}) = \left[\mathbf{J}_v(\mathbf{q})\mathbf{D}(\mathbf{q})^{-1}\mathbf{J}_v^T(\mathbf{q})\right]^{-1} \tag{11}$$

as detailed in e.g. [3] and [4]. In case of robots with non- or poorly backdrivable joints, arbitrarily large motor inertias can be added to the inertia matrix $\mathbf{D}(\mathbf{q})$ to simulate locked joints [15].

We now model the collision along unit direction $\mathbf{u}$ as a mass-spring system [16]

$$m_u(\mathbf{q})\ddot{x}_u(t') + k_u x_u(t') = f_{u,m} \tag{12}$$

with displacement x_u along $\mathbf{u}$, $t' := t - t_{\text{col}}$ introduced as shorthand, k_u stiffness of the contact and $f_{u,m}$ a (constant) braking force due to the robot's actuators. Note that we did not include damping as we do not want to dissipate energy. We aim at storing the collision energy to accelerate the arm when retracting with the object.

Initial conditions are $x_u(0) = x_{u,\text{col}}, \dot{x}_u(0) = \dot{x}_{u,\text{col}}$ where the former takes into account the spring pretension if relevant and the latter the impact velocity. This second order system can be solved analytically introducing natural frequency $\omega_n := \sqrt{k_u/m_u}$:

$$\begin{aligned} x_u(t') = {} & \frac{f_{u,m}}{k_u}\left[1 - \cos(\omega_n t')\right] \\ & + x_{u,\text{col}}\cos(\omega_n t') + \frac{\dot{x}_{u,\text{col}}}{\omega_n}\sin(\omega_n t') \end{aligned} \tag{13}$$

which results in the maximum collision force

$$f_{u,\max}(x_{u,\text{col}}, \dot{x}_{u,\text{col}}, m_u, k_u, f_{u,m}) = k_u x_u(t'_{\max}) \tag{14}$$

at time

$$t'_{\max} = \frac{1}{\omega_n}\arctan\left[\frac{\dot{x}_{u,\text{col}}}{\omega_n(x_{u,\text{col}} - f_{u,m}/k)}\right] \tag{15}$$

The gripper remains in contact as long as $x_u(t') \geqslant x_{u,\mathrm{col}}$ or equivalently if $t' \leqslant \Delta t'_{\mathrm{col}}$ with

$$\Delta t'_{\mathrm{col}} = \frac{1}{\omega_n} \arccos \left[\frac{\left(x_{u,\mathrm{col}} - \frac{f_{u,m}}{k_u}\right)^2 - \left(\frac{\dot{x}_{u,\mathrm{col}}}{\omega_n}\right)^2}{\left(x_{u,\mathrm{col}} - \frac{f_{u,m}}{k_u}\right)^2 + \left(\frac{\dot{x}_{u,\mathrm{col}}}{\omega_n}\right)^2} \right] \quad (16)$$

the total duration of contact.

D. Optimal choice of the impact impedance and velocity

We choose an initial k_u and $x_{u,\mathrm{col}}$ which are convenient sizewise to mechanically integrate into a gripper. Secondly, the pretension should be sufficient to keep the object in place during dynamic robot motion with the gripped object. Once k_u and $x_{u,\mathrm{col}}$ are chosen, the only key parameter left to set is the initial impact velocity, given $f_{u,m}$ is determined by the torque limits of the robot joints. Ideally the impact velocity is as high as possible in order to minimize the approach time as calculated in Eq. (8). Its maximum value should not result in a maximum collision force $f_{u,\max}$ exceeding what the object can handle. Nor should the collision force result in overloaded robot joints. We assume overload occurs if

$$\exists i : f_{u,\max} \left\{ \left| \mathbf{J}_v^T(\mathbf{q})\mathbf{u} \right| \right\}_i > \tau_{i,\max} \quad (17)$$

or stated otherwise if (at least) the i^{th} joint exceeds its hardware limit upon impact along $\mathbf{u}$ with collision force $\mathbf{f}_{\mathrm{ext}} = -f_{u,\max}\mathbf{u}$. Thirdly, the minimum duration of contact $\Delta t'_{\mathrm{col}}$ must be sufficient to build up vacuum and grip the object. A too long $\Delta t'_{\mathrm{col}}$ on the other hand introduces an unnecessary delay in the picking operation. Fourthly, the maximum spring compression $x_u(t')$ cannot be larger than allowed by the mechanical design. Equations (13), (14), (16) and (17) can be used to determine the maximum allowed impact velocity that does not violate any of these three constraints. If the initial values for k_u and $x_{u,\mathrm{col}}$ are not satisfactory, an additional design iteration might be necessary.

If one of these conditions is violated, either the object or the manipulator can be damaged. The latter can be avoided through overload clutching.

E. Overload protection through Series Clutched Actuation

While the high-speed picking strategy presented in the previous sections can be applied on a conventional high-speed industrial robot, there are some risks involved. Not much needs to go wrong to damage the robot as we are working close to the hardware limits, even in nominal operation. If e.g. a different object is present than expected and the collision occurs earlier at higher speed, the joints can be catastrophically overloaded. In order to solve this issue and obtain a more collision tolerant solution, the overload clutch technology presented in [10] and [11] can be used either in the manipulator arm or in the gripper itself. If an unexpected collision would occur, the overload clutches decouple, avoiding hardware damage. The presented planning and control strategy can be used as before, but with the clutch thresholds instead of the maximum intermittent joint torques. How this works in practice is demonstrated in the next section discussing the experimental validation.

IV. EXPERIMENTAL VALIDATION

A. Setup

The setup consists of a high-speed industrial robot fitted with series clutched actuators as shown in Fig. 1 and 4. Note that a conventional robot can also be used, although there is not much room for error in the latter case. Details on these clutches and their integrated joint torque sensors can be found in [10] and [11] respectively. Important to note is that the joint torque sensor in the i^{th} joint outputs two values: $\tau_{\mathrm{cdc,i}+}$ and $\tau_{\mathrm{cdc,i}-}$. In nominal operation with coupled clutches, $\tau_{\mathrm{cdc,i}+} = \tau_{\mathrm{cdc,i}-}$ while in a decoupled clutch, $\tau_{\mathrm{cdc,i}+} \neq \tau_{\mathrm{cdc,i}-}$. The latter can be used to distinguish between nominal, coupled clutch operation and a decoupled state after overload.

The robot is fitted with the custom compliant pneumatic gripper shown in Fig. 3. A contact time of $\Delta t_{\mathrm{col}} = 80$ ms was found to be sufficient to build up vacuum and grip the object. In the current setup, three springs in parallel are used resulting in a combined stiffness of $k_u = 3.9$ kN/m. The springs are precompressed by 30 mm resulting in an initial spring force of $f_{u,\mathrm{col}} = 117$ N. The shoulder joint –second closest to the robot's base– is actuated to approach the object. The joints closer to the end effector are assumed quasi-locked considering their limited backdrivability. Given the pose at the time of contact, the equivalent mass is calculated to be $m_u = 13.8$ kg. A braking force $f_{u,m}$ of -70 N can be exerted by the motors. Eqs. (13), (14), (16) and (17) suggest to limit the maximum allowed impact velocity $\dot{x}_{u,\mathrm{col}} \leqslant 0.65$ m/s.

B. Picking experiments

In a first experiment that serves as benchmark, the robot with suction cup contacts the object at zero velocity. The measurements are shown in Fig. 5(a). The robot's shoulder joint position, velocity, acceleration and motor torque are plotted as well as the readouts of a joint torque sensor integrated in the 5^{th} joint (wrist) and of a loadcell in between the object and the table. The joint profile consists of two parabolic blended trajectories as discussed in Section II. After contact is made at zero velocity and vacuum is achieved, the robot retracts with the object.

The high-speed variant is shown in Fig. 5(b). The time instant when contact with the object is made is indicated with a vertical dashed line. The movie still timings of the moment before contact Fig. 4(a), with the springs of the compliant gripper maximally compressed 4(b) and while retracting with the object 4(c) are also indicated. The object is picked while the robot speed is non-zero when making initial contact. The collision is detected, either by the loadcell or based on joint torque, using e.g. a (band-pass) momentum observer [17]. Upon detection, the arm is instructed to retract as fast as possible, constrained by the maximum acceleration $\ddot{q}_{\max}$. A reduction in picking time of 16% is achieved. The impact force when the springs are maximally compressed matches

Fig. 4: Movie stills of the high-speed picking experiment showing the robot with compliant pneumatic gripper (a) before contact, (b) with the springs of the compliant gripper maximally compressed and (c) while retracting, initially accelerated by the energy stored in the springs.

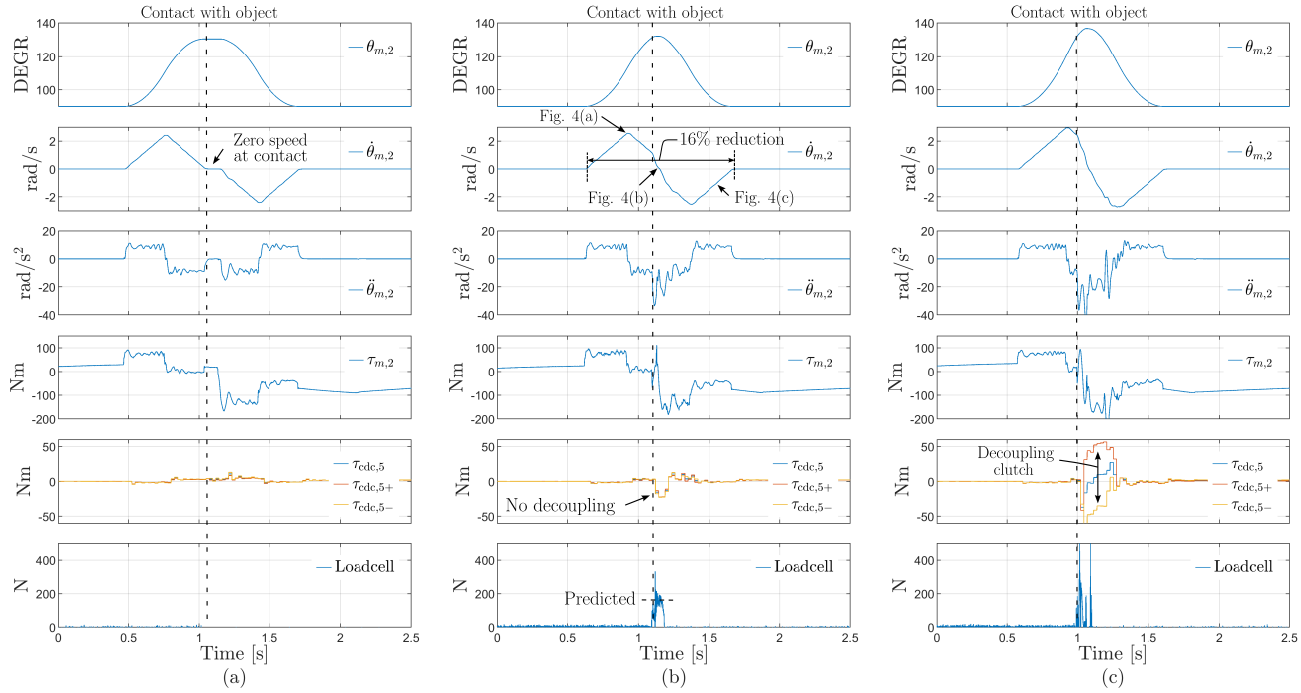

Fig. 5: Gripping experiments. Experiment (a) shows the benchmark where contact with the object is made at zero velocity. Experiment (b) shows the high-speed alternative where a compliant gripper contacts the object at non-zero velocity. The complete picking time is reduced by 16%. The time instants of the movie stills of Fig. 4 are indicated. In experiment (c), the collision velocity $\dot{x}_{u,\mathrm{col}}$ was too high resulting in (partial) decoupling of the overload clutch in the 5$^{\mathrm{th}}$ joint (wrist).

the $f_{u,\max} = 170$ N as predicted by the collision model of Section III, using the appropriate $\dot{x}_{u,\mathrm{col}}$, $f_{u,m}$, m_u and k_u.

If the impact velocity $\dot{x}_{u,\mathrm{col}}$ is higher, e.g. because of a miscalculation or by hitting a different than modeled object, the robot joints can be overloaded. In Fig. 5(c), the wrist joint torque sensor indicates decoupling of the overload clutch ($\tau_{\mathrm{cdc},5+} \neq \tau_{\mathrm{cdc},5-}$). While this robot can reset itself autonomously and continue operation at lower speed, a conventional robot would potentially be catastrophically damaged. Adding overload clutches (either in the arm or in the gripper itself) is hence recommended when using the presented compliant pneumatic gripper.

V. CONCLUSION

Industrial robots operate at ever increasing speeds. In fear of collision, they decelerate to a near standstill prior to interacting with the environment. To address this, a compliant pneumatic gripper and an impact-aware trajectory plan are presented to initiate contact at increased speed, all while staying within the mechanical limits of the system. Key parameters like the gripper's compliance and the maximum allowable initial collision velocity were identified, accompanied by recommendations on their optimal selection. The complete high-speed picking solution is experimentally validated. A significant 16% reduction in operation time was

achieved if contact is made at $\dot{x}_{u,\mathrm{col}} = 0.65$ m/s instead of at standstill.

REFERENCES

[1] N. Dehio, A. Kheddar. Robot-Safe Impacts with Soft Contacts Based on Learned Deformations. *IEEE International Conference on Robotics and Automation (ICRA)*, 2021.

[2] N. Dehio, Y. Wang, A. Kheddar. Dual-Arm Box Grabbing With Impact-Aware MPC Utilizing Soft Deformable End-Effector Pads. *IEEE Robotics and Automation Letters*, 7(2):5647–5654, 2022.

[3] O. Khatib. Inertial Properties in Robotic Manipulation: An Object-Level Framework. *International Journal of Robotics Research*, 14(1):19–36, 1994.

[4] Y. Wang, N. Dehio, and A. Kheddar. On Inverse Inertia Matrix and Contact-Force Model for Robotic Manipulators at Normal Impacts *IEEE Robotics and Automation Letters*, 7(2):3648–3655, 2022.

[5] F. Tassi, S. Gholami, S. Giudice, and A. Ajoudani. Impact Planning and Pre-configuration based on Hierarchical Quadratic Programming. *IEEE International Conference on Robotics and Automation*, 2022.

[6] D. Petkovic, N. D. Pavlovic, S. Shamshirband and N. B. Anuar. Development of a new type of passively adaptive compliant gripper. *Industrial Robot: An International Journal*, 40(6):610–623, 2013.

[7] Y–J. Kim, H. Song and C–Y. Maeng. BLT Gripper: An Adaptive Gripper With Active Transition Capability Between Precise Pinch and Compliant Grasp. *IEEE Robotics and Automation Letters*, 5(4):5518–5525, 2020.

[8] Y-F. Zheng, and H. Hemani. Mathematical Modeling of a Robot Collision with its Environment. *Journal of Robotic Systems*, 2(3):289–307, 1985.

[9] J. J. van Steen, N. van de Wouw and A. Saccon. Robot Control for Simultaneous Impact tasks via Quadratic Programming-based Reference Spreading. In *2022 American Control Conference (ACC)*, pages 3865–3872, 2022.

[10] F. Ostyn, T. Lefebvre, B. Vanderborght, and G. Crevecoeur. Overload clutch design for collision tolerant high–speed industrial robots. *IEEE Robotics and Automation Letters*, 6(2):863–870, 2021.

[11] F. Ostyn, B. Vanderborght, and G. Crevecoeur. Overload Clutch with Integrated Torque Sensing and Decoupling Detection for Collision Tolerant Hybrid High-Speed Industrial Cobots. *IEEE Robotics and Automation Letters*, 7(4):12601–12607, 2022.

[12] A. Bhatia, M. Johnson, and M.T. Mason. Direct drive hands: Force-motion transparency in gripper design. *Robotics: Sci. Syst.*, pages 1–33, 2019.

[13] F. Ostyn, B. Vanderborght, and G. Crevecoeur. Design and Control of a Quasi-Direct Drive Robotic Gripper for Collision Tolerant Picking at High Speed. *IEEE Robotics and Automation Letters*, 7(3):7692–7699, 2022.

[14] K.H. Mak, P. Xu, and J. Seo. High-Speed Scooping: An Implementation through Stiffness Control and Direct-Drive Actuation. *IEEE International Conference on Robotics and Automation (ICRA)*, 2023.

[15] P.M. Wensing, A. Wang, S. Seok, D. Otten, J. Lang, and S. Kim. Proprioceptive Actuator Design in the MIT Cheetah: Impact Mitigation and High-Bandwidth Physical Interaction for Dynamic Legged Robots. *IEEE Transactions on Robotics*, 33(3):509–522, 2017.

[16] J.K. Mills, and C.V. Nguyen. Robotic Manipulator Collisions: Modeling and Simulation. *Transactions of the ASME*, 114:650–659, 1992.

[17] J. Kim C. Cho, J. Song Y. Kim, and J. Kyung. Collision detection algorithm to distinguish between intended contact and unexpected collision. *Advanced Robotics*, 26:1–16, 2012.